Published in final edited form as:
Circ Cardiovasc Genet. 2014 October ; 7(5): 659–666. doi:10.1161/CIRCGENETICS.113.000504.

A Common Polymorphism in EC-SOD Affects Cardiopulmonary Disease Risk by Altering Protein Distribution

John M. Hartney, PhD[1,2,*], **Timothy Stidham, MD**[3,*], **David A. Goldstrohm, PhD**[1,*], **Rebecca E. Oberley-Deegan, PhD**[1], **Michael R. Weaver, BS**[1], **Zuzana Valnickova-Hansen, BSc**[4], **Carsten Scavenius, PhD**[4], **Richard K.P. Benninger, PhD**[3,5], **Katelyn F. Leahy, BS**[1], **Richard Johnson, BS**[3], **Fabienne Gally, PhD**[1], **Beata Kosmider, PhD**[1], **Angela K. Zimmermann, PhD**[6], **Jan J. Enghild, PhD**[4], **Eva Nozik-Grayck, MD**[3,*], and **Russell P. Bowler, MD, PhD**[1,*]

[1]Department of Medicine, National Jewish Health, University of Colorado Denver and National Jewish Health, Denver

[2]Integrated Department of Immunology, University of Colorado Denver and National Jewish Health, Denver

[3]Department of Pediatrics, University of Colorado School of Medicine, Aurora, CO

[4]Department of Molecular Biology and Genetics, Aarhus University, Aarhus, Denmark

[5]Department of Bioengineering, University of Colorado School of Medicine, Aurora, CO

[6]Institut de Biologie du Developpement de Marseille Luminy (IBDML), Aix-Marseille University, Marseille, France

Abstract

Background—The enzyme extracellular superoxide dismutase (EC-SOD; *SOD3*) is a major antioxidant defense in lung and vasculature. A nonsynonomous single nucleotide polymorphism (SNP) in EC-SOD (rs1799895) leads to an arginine to glycine (Arg->Gly) amino acid substitution at position 213 (R213G) in the heparin-binding domain (HBD). In recent human genetic association studies, this SNP attenuates the risk of lung disease, yet paradoxically increases the risk of cardiovascular disease.

Methods and Results—Capitalizing on the complete sequence homology between human and mouse in the HBD, we created an analogous R213G SNP knockin mouse. The R213G SNP did not change enzyme activity, but shifted the distribution of EC-SOD from lung and vascular tissue to extracellular fluid (e.g. bronchoalveolar lavage fluid (BALF) and plasma). This shift reduces susceptibility to lung disease (lipopolysaccharide-induced lung injury) and increases susceptibility to cardiopulmonary disease (chronic hypoxic pulmonary hypertension).

Conclusions—We conclude that EC-SOD provides optimal protection when localized to the compartment subjected to extracellular oxidative stress: thus, the redistribution of EC-SOD from

Correspondence: Russell Bowler, MD, PhD, National Jewish Health, 1400 Jackson Street, Room K715a, Denver, CO 80206, Tel: 303-398-1639, Fax: 303-270-2249, BowlerR@NJHealth.org.
*contributed equally

Conflict of Interest Disclosures: None

the lung and pulmonary circulation to the extracellular fluids is beneficial in alveolar lung disease but detrimental in pulmonary vascular disease. These findings account for the discrepant risk associated with R213G in humans with lung diseases compared with cardiovascular diseases.

Keywords

pulmonary hypertension; lung; antioxidant enzymes; cardiovascular disease

Introduction

In mammals, there are three superoxide dismutase (SOD) isoforms which constitute the major enzymatic antioxidant defense against superoxide. The extracellular isoform, EC-SOD or *SOD3*, is highly expressed in airways and lung epithelium and is the most abundant SOD in blood vessels. By reducing superoxide and oxidative stress, EC-SOD modulates multiple signaling pathways such as nitric oxide, NF-kappaB, Egr-1, and RhoA-dependent signal transduction [10–12]. In animal studies using knockout and overexpressing mice, EC-SOD attenuates oxidative stress and inflammation in the lungs from multiple inhaled toxins including LPS [4, 13–19]. Similarly, in the vasculature, EC-SOD preserves nitric oxide signaling, attenuates oxidative injury, and protects against vascular remodeling [20,3, 21, 22].

Because animal studies suggested a role for EC-SOD in cardiopulmonary disease, several groups have investigated EC-SOD gene associations in patients with heart and lung diseases. To date, 5 single nucleotide polymorphisms (SNPs) in EC-SOD (2 coding and 3 non-coding) have been associated with clinical outcomes in cardiovascular or pulmonary disease processes [23–27]. The nonsynonymous SNP (rs1799895) holds the most promise as a polymorphism that directly correlates with disease severity in humans and can provide insight into the mechanism for protection by EC-SOD. The rs1799895 SNP is a cytosine to guanine change at base pair +760 that results in an arginine to glycine substitution at amino acid 213 (R213G). The mean allele frequency of the R213G SNP is 4–6% in Asian populations and 2–3% in European populations [28, 29]. The R213G SNP was first reported to confer increased risk of ischemic heart disease in 9,188 participants from The Copenhagen City Heart Study[29]. Paradoxically, the R213G SNP was later found to reduce the risk of COPD and acute exacerbations of COPD in three independent, large population studies [23–25]. Because the R213G SNP only occurs in humans, we have limited experimental evidence and knowledge to explain this paradox of increased risk of vascular disease and reduced risk of pulmonary disease. From observational studies, we know that carriers of the R213G SNP have increased EC-SOD protein in plasma [30] and that the R213G variant EC-SOD protein has impaired *in vitro* binding to extracellular matrix elements [1]; however, we do not know how the R213G SNP changes the distribution of EC-SOD in tissue nor do we understand how the R213G SNP alters the response to lung and vascular injury *in vivo*.

Methods

Experimental animals: R213G SNP knockin mouse creation

The R213G knockin targeting vector was created using high fidelity Red/ET recombineering methods. Briefly, a 10.5 kb region was subcloned from a positively identified C57BL/6

BAC clone using homologous recombination. The short homology arm (SA) extended 2.25 kb 3′ to the LoxP-flanked Neo cassette and long homology arm (LA) extended 6.13 kb to the 3′-end of the single Lox P site. The single Lox P site is inserted upstream of exon 2 in intron 1–2, and the LoxP-flanked Neo cassette is inserted downstream of exon 2 in intron 2–3. The C -> G mutation (amino acid change: R>G) within exon 2 was generated by 3-step PCR mutagenesis. Using conventional sub cloning methods, the wild type sequence was replaced with the PCR fragment carrying the point mutation. Targeted iTL BA1 (C57BL/6N x 129/SvEv) hybrid embryonic stem cells were microinjected into C57BL/6 blastocysts. Resulting chimeras with a high percentage agouti coat color were mated to wild-type C57BL/6N mice to generate F1 heterozygous offspring. We obtained two independent C57BL/6 founder lines to generate homozygote R213G mice. DNA was sequenced periodically to verify lack of new spontaneous mutations. Animal experiments were approved by the Institutional Animal Care and Use Committee.

Southern blot analysis

DNA digested with BspEI was electrophoretically separated on a 0.8% agarose gel, transferred to a nylon membrane, and hybridized with a probe targeted against the 5′ external region of EC-SOD. DNA from C57BL/6, 129/SvEv, and BA1 (C57BL/6 x 129/SvEv) mice were used as wild-type controls.

Mouse DNA genotyping

R213G mice were genotyped using primers (Forward: 5′-AGGCTCAAGTCTGTGCCAGAAGG-3′, Reverse: 5′-TTTCCAATTCATTCACACACATGGG-3′) to distinguish wild type (357 bp amplicon) from knockin alleles (419 bp amplicon). DNA was amplified in genotyping PCR cocktail (10 mM primers, HiFi Buffer, 50 mM MgSO4, 10 mM DNTPs, HiFi Taq, water) by a 5 minute 99°C hot start for 30 cycles, 30 second 95°C denaturing, 30 second 55°C annealing, and 3 minute 68°C extending conditions. PCR products were run on a 1.5% agarose gel with a DNA ladder.

Human DNA genotyping

Lungs, graciously provided by Dr. Mason (National Jewish Health), were donated through the National Disease Research Interchange (NDRI, Philadelphia, PA) and International Institute for the Advancement of Medicine (IIAM, Edison, NJ) under a Human Subject Research exempt protocol. Isolated lung DNA (Qiagen DNA tissue kit) was screened for the R213G SNP using Real-time PCR allelic discrimination assay-by-design service and the TaqMan SNP Genotyping Assay for Human *SOD3* (C_2307506_10)(Applied Biosystems Life Technologies, Foster City, CA)

DNA sequencing

A DNA region containing the R213G SNP was sequenced using a forward primer (5′-AGGCTCAAGTCTG TGCCAGAAGG-3′) located in the long homology arm upstream of the R213G SNP and a reverse primer (5′-GGAACTTCGCTAGA CTAGTACGCGTG-3′) located within the Neo cassette downstream of the R213G SNP per established protocols

(Molecular Research Center, National Jewish Health). DNA was amplified and the PCR product sequenced on an ABI PRISM 3100 genetic analyzer. pGEM-3zf(+) DNA was used as a positive control.

EC-SOD activity assays

Pulverized lung (70 mg) was homogenized in SOD activity assay buffer and total lung protein concentration was determined by BCA protein assay (Pierce Biotechnology, Rockford, IL). EC-SOD was separated from intracellular SOD (SOD1 and SOD2) using the Glycoprotein Isolation Kit, ConA (Pierce Biotechnology) per manufacturer's instructions with the following minor modifications: spin columns contained 300 μl ConA Lectin Resin and the intracellular SOD fraction was collected prior to washing columns. Columns were incubated with 300 μl elution buffer for 15 minutes prior to collection of flow-through. Absence of EC-SOD in the intracellular SOD fraction was confirmed by western blot while eluted fractions containing EC-SOD were pooled and concentrated 10-fold using a centriprep concentrator (Amicon-ultracel-10K, Millipore). Activity levels were measured by the SOD assay kit-WST (Dojindo Molecular Technologies, Maryland, USA), according to manufacturer's instructions. Data were expressed as units of EC-SOD activity per mg of total lung protein.

Heparin-sepharose binding

Pooled plasma or lung tissue from ten mice (wild type or R213G) was homogenized and centrifuged; and supernatant dialyzed against 20 mM Tris –HCl pH 7.5 [1]. Following dialysis, the sample was applied to 1ml HiTrap Heparin Sepharose (GE Healthcare) and heparin-binding proteins eluted with a linear gradient of NaCl (0 mM±1 M) in 50 mM Tris-HCl, pH 7.5 at a flow rate of 1ml/min. Fractions were analyzed for EC-SOD activity by inhibition of cytochrome c reduction as described previously [2]. To test if the R213G SNP altered SOD activity, we normalized activity to the relative EC-SOD content in the peak fraction. We determined the relative EC-SOD content by western blotting using a polyclonal rabbit murine EC-SOD antibody and Cy5 labeled anti-rabbit secondary antibody (Sigma).

Histological analysis

EC-SOD immunostaining was performed as previously described using mouse- or human-specific antibodies. [3,4,5]. Mouse lungs were inflated-fixed at 25 cm H_20 pressure with 4% paraformaldehyde. EC-SOD KO and wild type mice were used as negative and positive controls respectively.

Bronchoalveolar lavage

Lungs were lavaged with 1 mL PBS and 20 μl of total bronchoalveolar lavage fluid (BALF) was diluted in 10 mL Isoton II diluent and counted on a Z2 particle count and size analyzer (Beckman Coulter, Fullerton, CA).

Western blot analysis

Homogenized lung tissue was run on a 12% Tris/Glycine SDS-PAGE gel and transferred to PVDF membrane per standard protocols [6]. Blots were incubated with primary antibody as

follows: Beta-actin 1:20,000 (Sigma, St. Louis, MO), EC-SOD 1:1000 (8130), 4-HNE 1:1000 (Abcam, Cambridge, MA), nitrotyrosine 1:500 (UpState, Lake Placid, NY). Following incubation with secondary antibody, blots were developed with ECL Plus (GE), imaged with STORM 860 (GE) using the fluorescent blue (430nm) setting, quantified using ImageQuant software, and expressed relative to beta-actin.

Gene expression

Total RNA was extracted using either TRIzol (Invitrogen, Carslbad CA) or RNeasy kit (Qiagen) according to the manufacturer's instructions and differences in gene expression were determined using Real-Time RT-PCR as previously described [7]. Gene expression was determined using comparative threshold cycle ($\Delta\Delta C_T$) as suggested by the manufacturer (Applied Biosystems, Foster City, CA) normalizing each sample to 18s rRNA. The following primer sets were purchased from Assays on Demand (Applied Biosystems); 18s rRNA (cat#4310893E), *SOD3* (Mm01213380-s1), *SOD1* (Mm01700393_g1) and *SOD2* (Mm00449726_m1).

Proinflammatory cytokine and chemokine measurements

Cytokine and chemokine concentrations in mouse lung tissue and BALF were measured (ELISA TECH, Aurora, CO) using either the MSD mouse proinflammatory 7-plex ultra-sensitive kit or the proinflammatory panel 1 V-PLEX kit (Meso Scale Discovery, Gaithersburg, MD) per manufacturer's instructions.

Total differential cell counts

Total BALF was centrifuged for 15 minutes at 300 × g. The cell pellet was resuspended in 200 ul PBS. 180 ul was spotted to glass slides and allowed to dry overnight. Slides were then stained for differential cell counts using HEMA 3 stain per manufacturer's instruction (Fisher Scientific, Kalamazoo, MI).

Chronic hypoxic pulmonary hypertension

Four week old WT C57/BL6 and HM R213G mice were exposed to hypobaric hypoxia (395 torr) for 35 days: chambers simulated altitude (5486 m) equivalent to 10% oxygen. Normoxic control mice were maintained in Denver ambient air (1,609 m).

Isolation of pulmonary arteries

Lungs were perfused with a slurry of iron particles in warmed agarose and minced; iron-containing PAs were separated from lung parenchyma by magnet.[8] The PA was digested with collagenase to release the iron particles, and the isolated PA tissue homogenized and sonicated in RIPA buffer for western blots.

Assessment of pulmonary hypertension

Right ventricular systolic pressure (RVSP) was measured in anesthetized mice by direct RV puncture through a closed chest using the Cardiomax III Cardiac Output system (Columbus Instruments) as previously described [7]. Right ventricular hypertrophy (RVH) was determined as the ratio of right ventricular/left ventricular + septum weights (RV/LV+S).

Assessment of pulmonary vascular remodeling

To evaluate hypoxia-induced muscularization of small vessels, lung sections were stained with mouse monoclonal α-smooth muscle actin antibody (α-SMA)(1:100, Clone 1A4) and the number of positively stained small vessels (<50 um) determined as previously described[7]. Collagen deposition was evaluated using non-linear Second Harmonic Generation (SHG) imaging, based on the ability of collagen fibrils to intrinsically generate an SHG signal [9]. 100μm lung sections were deparaffinized and imaged on an LSM510-Meta microscope (Zeiss, Jena, Germany) with a 63× 1.4NA Plan-Apochromat oil immersion objective, using a 800nm mode-locked 100fs-pulsed Ti:sapphire laser (Chameleon, Coherent) for non-linear excitation. SHG was detected with a narrow band 390–410nm band-pass filter (Chroma) and autofluroescence was detected with a 450–700nm broad band pass filter. Settings were kept constant between experiments. Pulmonary arteries <200 μm diameter associated with bronchioles were imaged (n=5 per mouse). To quantify collagen, the area of SHG signal around a single pulmonary artery, measured as pixels, was calculated and expressed relative to the vessel perimeter. All image analyses were performed by an investigator blinded to treatment groups using Matlab (Mathworks) and ImageJ (NIH, Bethesda, MD). Analyses

Statistical analysis

Results are presented as the means ± standard error (SE). A Kruskal-Wallis test and Wilcoxon rank-sum test were performed to determine whether the groups were significantly different. A value of $P < 0.05$ was considered statistically significant.

Results

Translating human SNP association studies into animals can be challenging for two reasons: first, the genetic component for most common diseases are poorly modeled by knockout and overexpressing mice; second, genetic background differences often make a relevant translation of a human SNP into a mouse impossible. For instance, many human disease SNPs do not change protein sequence (i.e. are synonymous or in regulatory or unknown element of the gene); thus, are difficult to translate onto the mouse genome. Fortunately, the R213G SNP lies in the extracellular matrix-binding domain (ECM-BD) coding region of exon 2, a region that is 100% conserved between mice and humans (Fig. 1A). Therefore, we were able to clone a single base cytosine to guanine substitution at the equivalent R213G position (Fig. 1B**,** red asterisk) into the native mouse SOD3 to mimic the naturally occurring R213G SNP in humans. After target insertion, we obtained 4 positive clones that were confirmed for proper homologous integration by Southern blot (Fig. 1C). Positive mice and their offspring were further confirmed by genotyping (Fig. 1D) and DNA sequencing (Fig. 1E). Similar to humans[30], mice with the R213G SNP have high levels of EC-SOD protein and activity in plasma (Fig. 1F & G; P = 0.01). The R213G EC-SOD in plasma has reduced heparin-binding affinity compared to wild type protein (Fig. 1H); however, the purified wild type and R213G EC-SOD had similar SOD activity per unit of purified protein (Fig. 1I). Although human studies have shown that presence of the R213G SNP is associated with 2–4 fold increased EC-SOD protein in plasma [30] and the R213G variant EC-SOD protein has impaired *in vitro* binding to extracellular matrix elements [1], there are no reports of the

effects of R213G SNP on tissue distribution of EC-SOD. To study tissue distribution of EC-SOD in lung parenchyma and vasculature for the R213G SNP *in vivo*, we performed both immunolocalization and western blotting. Furthermore, to determine whether the R213G knockin mice accurately recapitulate R213G human carriers, we screened 78 unique lung samples from a human biobank to identify 2 humans heterozygous for the R213G SNP. By immunolocalization, the R213G SNP in mice was associated with a distinct reduction in staining for EC-SOD in lung parenchyma, pulmonary vasculature (Fig. 1J), and aorta (Fig. 1K). On quantitative western blots of lung (Fig. 1L) EC-SOD protein was reduced by 72% in the R213G mice ($p=0.03$) with corresponding reduction in EC-SOD activity assays (Fig. 1M). This marked decrease in lung EC-SOD content in R213G mice was recapitulated in humans who carried the R213G SNP (Fig. 1N). Notably, we also discovered that the R213G SNP was associated with higher EC-SOD in the bronchoalveolar lining fluid (BALF) in both mice (Fig. 1O; $P = 0.01$) and humans (Fig. 1P). No compensatory gene expression changes were observed in other superoxide dismutase enzymes (*SOD1* or *SOD2*) in the lungs of R213G mice (data not shown). A small but significant increase in *SOD3* expression was detected in whole lung tissue but not in isolated vascular tissue (Supplemental Fig. 1A–B). Thus, these findings demonstrate that the presence of the R213G polymorphism is sufficient to alter the distribution of EC-SOD protein from lung and vascular tissue to extracellular fluids such as BALF and plasma.

Since human gene association studies suggested the R213G SNP was associated with lower rates of lung inflammation (acute exacerbations of COPD) and animal studies using EC-SOD knockout and overexpressing mice have shown that EC-SOD protects the lung from multiple inflammatory and oxidative stress insults[15], we postulated that the high levels of EC-SOD in the BALF associated with the R213G SNP would protect mice from LPS-induced acute lung injury. One day after exposure to LPS, mice with the R213G SNP had a trend toward fewer BALF total cells (Fig. 2A; $P = 0.2$), and significantly fewer neutrophils (Fig. 2B; $P = 0.03$). The number of macrophages recovered from BALF did not significantly differ between groups at any time point assessed (Fig. 2C). Additionally there were significantly less pro-inflammatory cytokines (TNF-α, KC, and IL-12p70) in BALF after LPS exposure (Fig. 2D). Measurement of these same mediators in homogenized lung tissue revealed no difference between WT and R213G samples at any of the time points assessed (Supplemental Fig. 1C). Similarly while LPS inhalation induces a significant increase in total BALF protein in both genotypes the R213G samples were not significantly different from the respective WT samples (Supplemental Fig. 1D). Finally there a trend toward significantly less oxidative stress in the lung tissue of R213G mice after LPS compared to WT mice as measured by western blot of 4-HNE (Fig. 2E; $P = 0.1$). The attenuation of oxidative stress occurred despite the decreased content of lung EC-SOD, which suggests that high levels of EC-SOD in airway fluids (rather than lung tissue) are sufficient to reduce oxidative stress from toxic inhalations. These data strongly suggest that people with the R213G polymorphism are likely protected from inhalational lung injury due to high levels of EC-SOD in their bronchoalveolar fluid.

In contrast to reduced risk of lung disease, the R213G SNP has been associated with increased risk of cardiovascular disease. The mechanism for this increased risk is unknown,

but our findings indicate that the R213G SNP leads to a marked depletion of EC-SOD in the walls of blood vessels (Fig. 1K). To determine if the R213G SNP increases susceptibility to vascular injury, we evaluated the impact of the R213G SNP on the development of pulmonary vascular disease due to chronic hypoxia (hypoxia induced pulmonary hypertension (PH)). By western blot, EC-SOD protein was dramatically reduced in isolated pulmonary arteries from R213G mice (Fig. 3A). Compared to wild type littermates, mice with the R213G SNP exhibited PH at baseline and had worsened chronic hypoxic PH, shown by elevated right ventricular systolic pressure (Fig. 3B; $P = 0.0007$) and hypertrophy (Fig. 3C; $P = 0.0007$). The increased PH in the R213G SNP mice was associated with increased medial wall remodeling as measured by an increased number of muscularized vessels (< 50 micron) identified by positive α-smooth muscle-actin immunostaining (Fig. 3D and E; $P = 0.03$). The R213G mice also display increased hypoxia-induced pulmonary artery adventitial remodeling, as demonstrated by enhanced perivascular collagen deposition (Fig. 3F and G; $P = 0.002$). These results indicate that increased risk of vascular disease in people with the R213G SNP is due to reduced EC-SOD in blood vessels.

Discussion

The human, R213G SNP (rs1799895) is associated with increased risk of cardiovascular disease and reduced risk of airway disease in multiple large genetic association studies. In this study, we show that the SNP results in reduced binding to heparin, but no loss of enzymatic activity. The reduced binding to heparin and other matrix elements is most likely due to changing the codon from arginine to glycine for a key amino acid in the extracellular matrix binding domain of the protein. We are the first to show that this results in reduced EC-SOD protein and activity in both human lung and vascular tissue, but leads to increased EC-SOD in extracellular fluid such as plasma and lung epithelial lining fluid.

The benefit of a shift of EC-SOD protein from tissue to extracellular fluid such as the lung epithelial lining fluid is that there is reduced lung inflammation after inhalation of pro-oxidants such a LPS. The increased superoxide dismutase activity in the epithelial lining fluid leads to a reduction in proinflammatory cytokines and inflammatory cells. This attenuation in inflammation outweighs the potential loss of EC-SOD activity in the lung tissue. The consequences of reduced EC-SOD in vascular tissue is more significant in oxidative stress dependent vascular injury models such as hypoxia induced-PH. The increased susceptibility to vascular injury models should not be surprising since the R213G SNP results in marked depletion of EC-SOD in blood vessels, in which EC-SOD is normally the most abundant antioxidant enzyme. Thus, carriers of the human R21G polymorphism and its murine equivalent mouse have a phenotype similar to an EC-SOD overexpressor mouse in the epithelial lining fluid, but a EC-SOD knock out in tissue. These paradoxical effects are consistent with animal models in which show that EC-SOD overexpressing mice are protective of LPS and other inhalational injury, while EC-SOD knockout mice are more sensitive to cardiovascular injury such as hypoxia-induced PH and ischemia reperfusion.

The teleological explanation for persistence of the SNP in northern European (MAF 2–3%) and Asian populations (MAF ~ 6%) is unknown. We speculate that increased EC-SOD in lung lining fluid may serve to attenuate chronic lung inflammation from indoor air pollution

(i.e. indoor cooking). This benefit would have to lead to reproductive advantages compared to the increase susceptibility to cardiovascular disease.

In summary, the human R213G SNP is one of only a few SNPs that have been reproducibly linked with cardiopulmonary disease and also one of the few SNPs that can be faithfully translated into a mouse model. Our findings demonstrate that humans and mice with the R213G SNP have a shift in distribution of EC-SOD protein from lung and vascular tissue into extracellular fluids. This altered distribution increases the amount of SOD activity in lung lining fluid and reduces SOD activity in lung tissue and blood vessels (Fig. 4). This shift explains the paradox of how a single polymorphism can simultaneously reduce the risk for lung disease while increasing the risk of vascular disease. The benefits of reducing the risk of lung injury from inhaled agents may provide a teleological explanation for why the R213G SNP is common in humans despite its concurrent increased susceptibility for vascular disease.

Supplementary Material

Refer to Web version on PubMed Central for supplementary material.

Acknowledgments

We would like to thank the contributions from the following individuals: Tim Oury for supplying the primary antibody for immunostaining, Steen V. Petersen and Peter Henson for critical review and discussions of the manuscript, Robert Mason, for access to human lung tissue and BALF, Radu Moldovan for expert help with TPE-SHG, Sean Jacobson for running non-parametric statistics, and Boyd Jacobson and Katherine Neville for help in the illustration of the mechanism figure.

Funding Sources: This work was supported by the Flight Attendants Medical Research Institute (FAMRI 09_2050) and National Institute of Health (NIH HL111288, RB and HL086680, EG). TPE-SHG experiments were performed in the University of Colorado Anschutz Medical Campus Advance Light Microscopy Core supported in part by NIH/NCRR Colorado CTSI Grant Number UL1 RR025780.

References

1. Petersen SV, Olsen DA, Kenney JM, Oury TD, Valnickova Z, Thogersen IB, et al. The high concentration of arg213-->gly extracellular superoxide dismutase (ec-sod) in plasma is caused by a reduction of both heparin and collagen affinities. Biochem J. 2005; 385:427–432. [PubMed: 15362977]
2. Oury TD, Crapo JD, Valnickova Z, Enghild JJ. Human extracellular superoxide dismutase is a tetramer composed of two disulphide-linked dimers: A simplified, high-yield purification of extracellular superoxide dismutase. Biochem J. 1996; 317(Pt 1):51–57. [PubMed: 8694786]
3. Nozik-Grayck E, Suliman HB, Majka S, Albietz J, Van Rheen Z, Roush K, et al. Lung ec-sod overexpression attenuates hypoxic induction of egr-1 and chronic hypoxic pulmonary vascular remodeling. Am J Physiol Lung Cell Mol Physiol. 2008; 295:L422–430. [PubMed: 18599502]
4. Bowler RP, Nicks M, Warnick K, Crapo JD. Role of extracellular superoxide dismutase in bleomycin-induced pulmonary fibrosis. Am J Physiol Lung Cell Mol Physiol. 2002; 282:L719–726. [PubMed: 11880297]
5. Oury TD, Schaefer LM, Fattman CL, Choi A, Weck KE, Watkins SC. Depletion of pulmonary ec-sod after exposure to hyperoxia. Am J Physiol Lung Cell Mol Physiol. 2002; 283:L777–784. [PubMed: 12225954]
6. Villegas LR, Kluck D, Field C, Oberley-Deegan RE, Woods C, Yeager ME, et al. Superoxide dismutase mimetic, mnte-2-pyp, attenuates chronic hypoxia-induced pulmonary hypertension,

pulmonary vascular remodeling, and activation of the nalp3 inflammasome. Antioxid Redox Signal. 2013; 18:1753–1764. [PubMed: 23240585]

7. Hartney JM, Brown J, Chu HW, Chang LY, Pelanda R, Torres RM. Arhgef1 regulates alpha5beta1 integrin-mediated matrix metalloproteinase expression and is required for homeostatic lung immunity. Am J Pathol. 2010; 176:1157–1168. [PubMed: 20093499]
8. Waypa GB, Chandel NS, Schumacker PT. Model for hypoxic pulmonary vasoconstriction involving mitochondrial oxygen sensing. Circ Res. 2001; 88:1259–1266. [PubMed: 11420302]
9. Lim RS, Kratzer A, Barry NP, Miyazaki-Anzai S, Miyazaki M, Mantulin WW, et al. Multimodal cars microscopy determination of the impact of diet on macrophage infiltration and lipid accumulation on plaque formation in apoe-deficient mice. J Lipid Res. 2010; 51:1729–1737. [PubMed: 20208058]
10. Richens TR, Linderman DJ, Horstmann SA, Lambert C, Xiao YQ, Keith RL, et al. Cigarette smoke impairs clearance of apoptotic cells through oxidant-dependent activation of rhoa. Am J Respir Crit Care Med. 2009; 179:1011–1021. [PubMed: 19264974]
11. Bowler RP, Barnes PJ, Crapo JD. The role of oxidative stress in chronic obstructive pulmonary disease. Copd. 2004; 1:255–277. [PubMed: 17136992]
12. Jung O, Marklund SL, Geiger H, Pedrazzini T, Busse R, Brandes RP. Extracellular superoxide dismutase is a major determinant of nitric oxide bioavailability: In vivo and ex vivo evidence from ecsod-deficient mice. Circ Res. 2003; 93:622–629. [PubMed: 12933702]
13. Bowler RP, Arcaroli J, Crapo JD, Ross A, Slot JW, Abraham E. Extracellular superoxide dismutase attenuates lung injury after hemorrhage. Am J Respir Crit Care Med. 2001; 164:290–294. [PubMed: 11463603]
14. Bowler RP, Arcaroli J, Abraham E, Patel M, Chang LY, Crapo JD. Evidence for extracellular superoxide dismutase as a mediator of hemorrhage-induced lung injury. Am J Physiol Lung Cell Mol Physiol. 2003; 284:L680–687. [PubMed: 12618426]
15. Bowler RP, Nicks M, Tran K, Tanner G, Chang LY, Young SK, et al. Extracellular superoxide dismutase attenuates lipopolysaccharide-induced neutrophilic inflammation. Am J Respir Cell Mol Biol. 2004; 31:432–439. [PubMed: 15256385]
16. Tollefson AK, Oberley-Deegan RE, Butterfield KT, Nicks ME, Weaver MR, Remigio LK, et al. Endogenous enzymes (nox and ecsod) regulate smoke-induced oxidative stress. Free Radic Biol Med. 2010; 49:1937–1946. [PubMed: 20887783]
17. Yao H, Arunachalam G, Hwang JW, Chung S, Sundar IK, Kinnula VL, et al. Extracellular superoxide dismutase protects against pulmonary emphysema by attenuating oxidative fragmentation of ecm. Proc Natl Acad Sci U S A. 2010
18. Ghio AJ, Suliman HB, Carter JD, Abushamaa AM, Folz RJ. Overexpression of extracellular superoxide dismutase decreases lung injury after exposure to oil fly ash. Am J Physiol Lung Cell Mol Physiol. 2002; 283:L211–218. [PubMed: 12060579]
19. Kang SK, Rabbani ZN, Folz RJ, Golson ML, Huang H, Yu D, et al. Overexpression of extracellular superoxide dismutase protects mice from radiation-induced lung injury. Int J Radiat Oncol Biol Phys. 2003; 57:1056–1066. [PubMed: 14575837]
20. Oury TD, Ho YS, Piantadosi CA, Crapo JD. Extracellular superoxide dismutase, nitric oxide, and central nervous system o2 toxicity. Proc Natl Acad Sci U S A. 1992; 89:9715–9719. [PubMed: 1329105]
21. Hartney T, Birari R, Venkataraman S, Villegas L, Martinez M, Black SM, et al. Xanthine oxidase-derived ros upregulate egr-1 via erk1/2 in pa smooth muscle cells; model to test impact of extracellular ros in chronic hypoxia. PLoS ONE. 2011; 6:e27531. [PubMed: 22140445]
22. Xu Y, Stenmark KR, Das M, Walchak SJ, Ruff LJ, Dempsey EC. Pulmonary artery smooth muscle cells from chronically hypoxic neonatal calves retain fetal-like and acquire new growth properties. Am J Physiol. 1997; 273:L234–245. [PubMed: 9252561]
23. Juul K, Tybjaerg-Hansen A, Marklund S, Lange P, Nordestgaard BG. Genetically increased antioxidative protection and decreased chronic obstructive pulmonary disease. Am J Respir Crit Care Med. 2006; 173:858–864. [PubMed: 16399992]

24. Young RP, Hopkins R, Black PN, Eddy C, Wu L, Gamble GD, et al. Functional variants of antioxidant genes in smokers with copd and in those with normal lung function. Thorax. 2006; 61:394–399. [PubMed: 16467073]

25. Siedlinski M, van Diemen CC, Postma DS, Vonk JM, Boezen HM. Superoxide dismutases, lung function and bronchial responsiveness in a general population. Eur Respir J. 2009; 33:986–992. [PubMed: 19213780]

26. Dahl M, Bowler RP, Juul K, Crapo JD, Levy S, Nordestgaard BG. Superoxide dismutase 3 polymorphism associated with reduced lung function in two large populations. Am J Respir Crit Care Med. 2008; 178:906–912. [PubMed: 18703790]

27. Sorheim IC, DeMeo DL, Washko G, Litonjua A, Sparrow D, Bowler R, et al. Polymorphisms in the superoxide dismutase-3 gene are associated with emphysema in copd. COPD. 2010; 7:262–268. [PubMed: 20673035]

28. Marklund SL, Nilsson P, Israelsson K, Schampi I, Peltonen M, Asplund K. Two variants of extracellular-superoxide dismutase: Relationship to cardiovascular risk factors in an unselected middle-aged population. J Intern Med. 1997; 242:5–14. [PubMed: 9260561]

29. Juul K, Tybjaerg-Hansen A, Marklund S, Heegaard NH, Steffensen R, Sillesen H, et al. Genetically reduced antioxidative protection and increased ischemic heart disease risk: The copenhagen city heart study. Circulation. 2004; 109:59–65. [PubMed: 14662715]

30. Sandstrom J, Nilsson P, Karlsson K, Marklund SL. 10-fold increase in human plasma extracellular superoxide dismutase content caused by a mutation in heparin-binding domain. J Biol Chem. 1994; 269:19163–19166. [PubMed: 8034674]

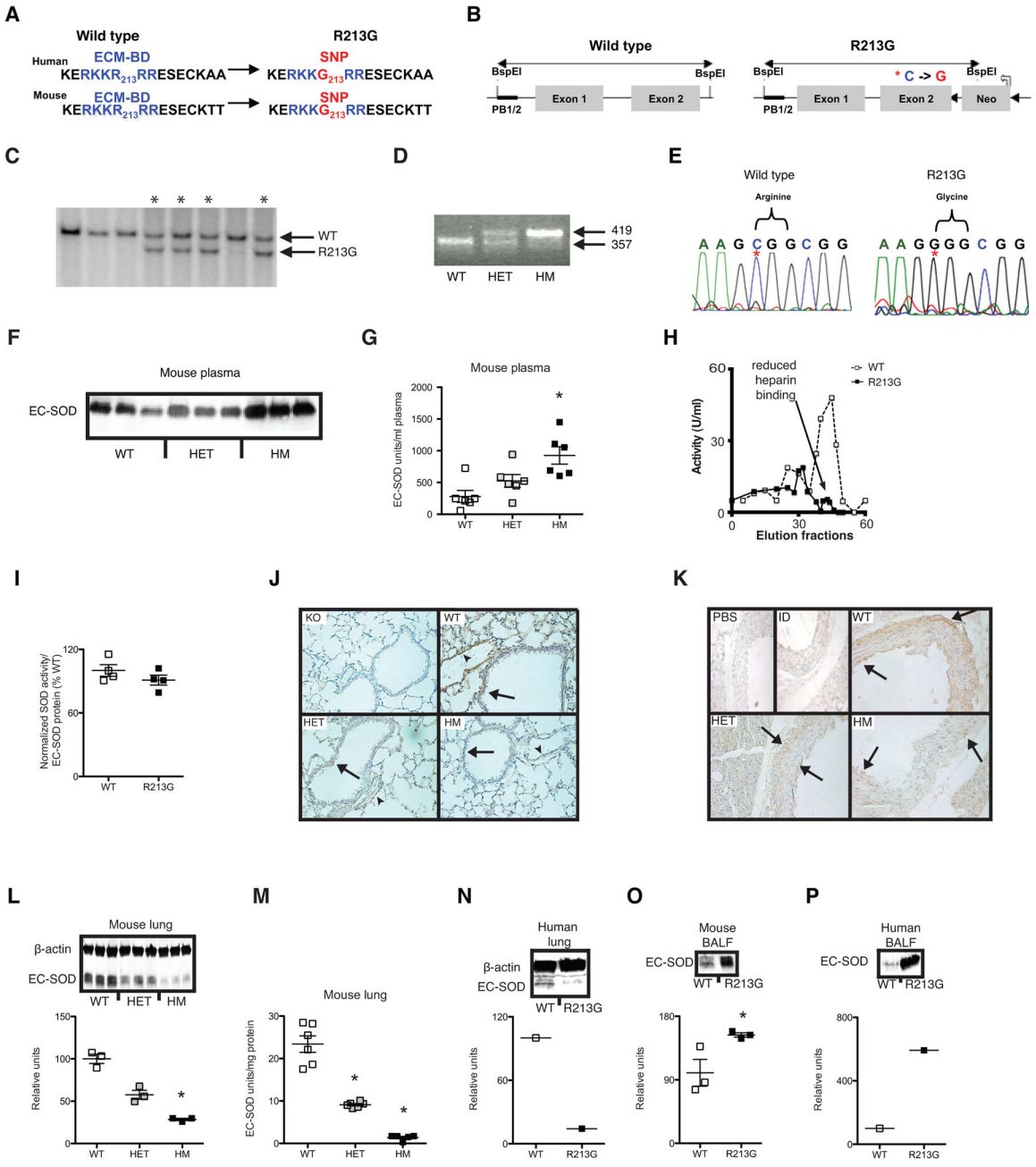

Figure 1.

Characterization of R213G SNP knockin mouse. (**A**) Homologous recombination introduces the identical R213G (C→G) SNP resulting in an identical arginine to glycine amino acids substitution in the extracellular matrix-binding domain (ECM-BD) of EC-SOD. Blue amino acids represent the conserved ECM-BD region and red represent R213G SNP at position 213. (**B**) R213G SNP homologous recombinant containing a Neo cassette (Neo). Red asterisk is site of R213G SNP. Black triangles are LoxP sites. PB ½ is probe site for Southern blots. (**C**) Confirmation of R213G positive clones (asterisks) by Southern blot. (**D**) R213G mouse DNA genotyping. Wild type (WT) mice produce a 357 bp amplicon, R213G

heterozygous (HET) mice produce both a 357 bp and 419 bp amplicon, and R213G homozygous (HM) mice produce 419 bp amplicon. (**E**) DNA sequence confirms C→G mutation (red asterisk) changing the codon from CGG (Arginine) to GGG (Glycine). (**F**) Plasma EC-SOD protein of WT, HET and HM mice. (**G**) EC-SOD activity in units per ml of plasma (n = 6 for all genotypes). (**H**) Heparin sepharose binding using purified EC-SOD from wild type (WT, n = 1) open squares and dashed line) and R213G homozygous (R213G, n = 1) mouse (black squares and solid line) in units/ml (U/ml) of elution volume. (**I**) SOD activity normalized to protein (n =3 for both WT and R213G). (**J**) EC-SOD immunostaining in murine lung tissue. Brown staining (arrow = airway, arrowhead = vessel) for wild type (WT), R213G heterozygous (HET) and R213G homozygous (HM) mice. EC-SOD knockout mice (KO) were used as background EC-SOD staining controls. (**K**) EC-SOD immunostaining in mouse aorta. Brown staining (arrows) shows EC-SOD localization for WT, HET and HM mice. EC-SOD immunodepleted (ID) and Phosphate buffered saline (PBS) were used for nonspecific background staining detection. (**L**) EC-SOD total protein was analyzed in total lung tissue by western blot from WT (n = 3), HET (n = 3) and HM (n =3) animals. (**M**) EC-SOD activity in units per mg of lung tissue protein of WT (n = 6), Het (n = 6) and HM (n = 5) mice. (**N**) EC-SOD protein in lung tissue from WT and R213G human carrier. (**O**) EC-SOD protein in bronchoalveolar lavage fluid (BALF) of wild type (WT) and R213G homozygous (R213G) mice. (**P**) EC-SOD protein in BALF from WT and R213G human carrier obtained post-mortem. Data are shown as mean ± S.E. * $P < 0.05$ compared to WT.

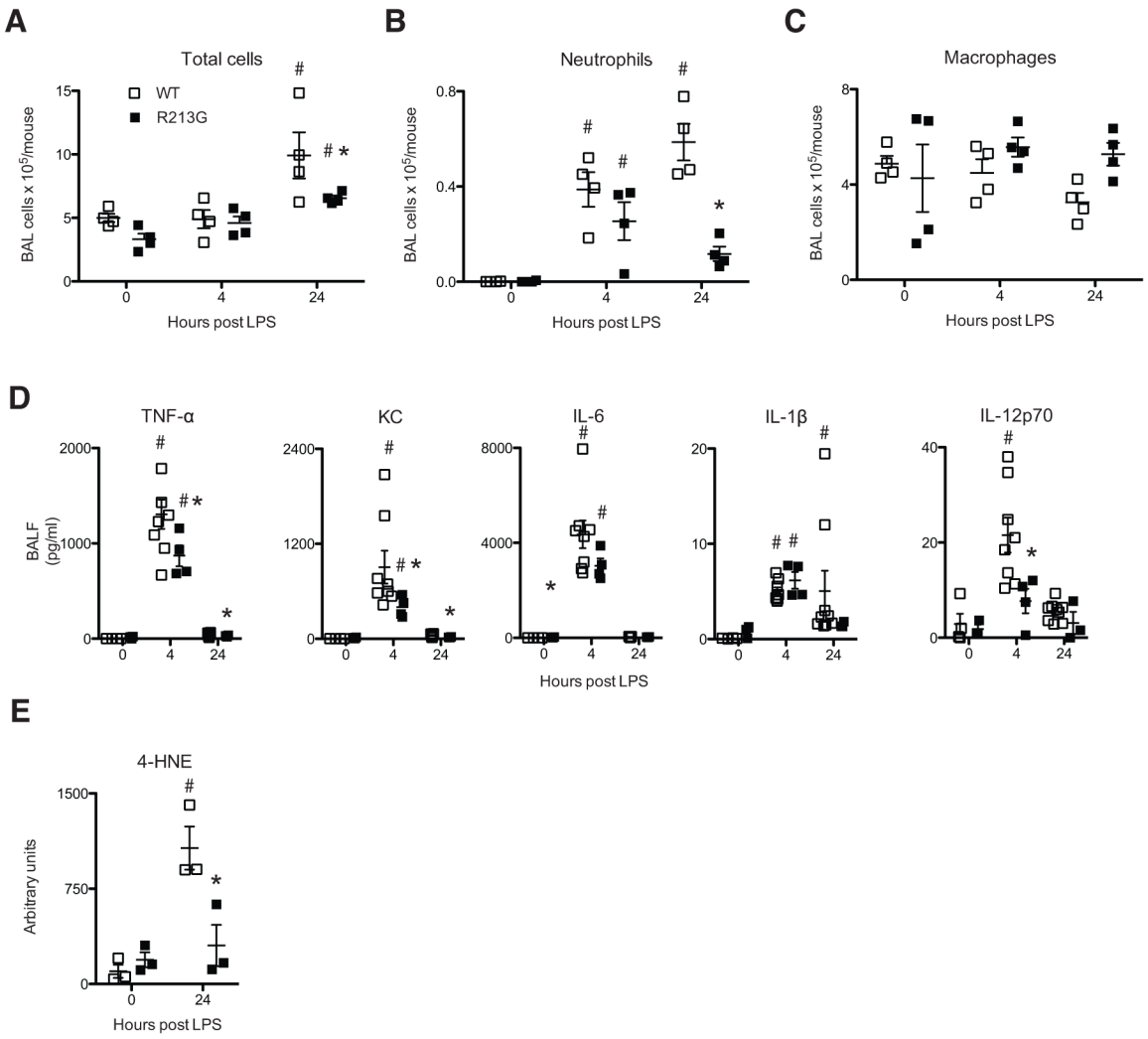

Figure 2.

Mice with R213G SNP have attenuated injury to inhaled LPS. (**A**) Total cells counts in BALF 0, 4 and 24 hours post-LPS. (n = 4 per group). (**B**) Total neutrophil counts in BALF (**C**) Total macrophages counts in BALF. (**D**) Cytokines in BALF of WT and R213G animals at 0 hours (WT n = 4, R213G n = 3), 4 hours (WT n = 8, R213G n= 4) and 24 hours (WT n = 9, R213G n = 4) post LPS inhalation. (**E**) 4-HNE in lung tissue. Data are presented as mean ± S.E. # $P < 0.05$ compared to samples at 0 hours for each genotype. * $P < 0.05$ comparing WT to R213G samples under identical conditions.

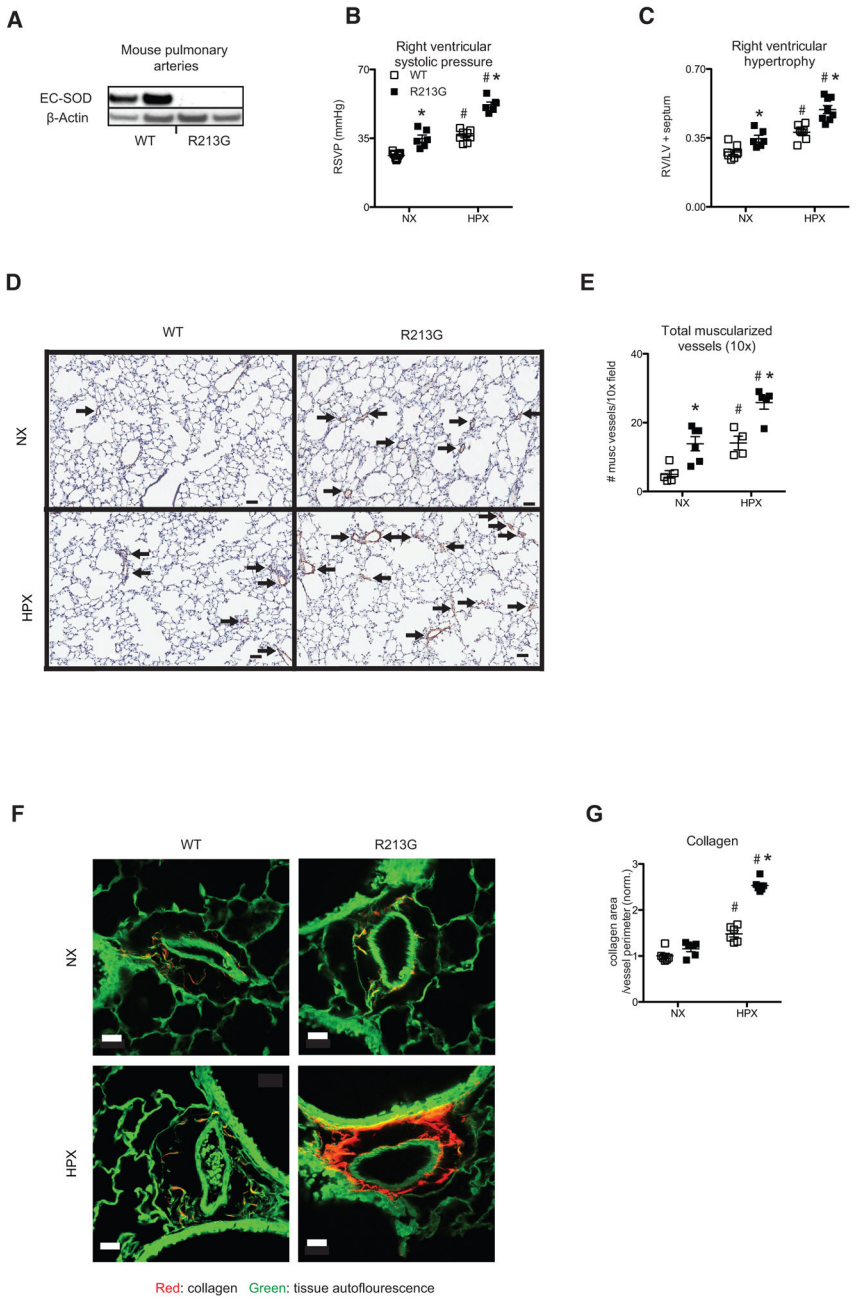

Figure 3.

R213G SNP reduces vascular EC-SOD and increases susceptibility to pulmonary hypertension. (**A)** EC-SOD protein expression in pulmonary artery tissue isolated from normoxic (NX) wild type (WT) and R213G homozygous mice (R213G). (**B**) Right ventricular systolic pressure (RVSP mmHg) at baseline (WT n = 9, R213G n = 6) and after 35 days of chronic hypoxia (HPX) in WT (n = 8) and R213G (n = 6). (**C**) Right ventricular hypertrophy (RV/LV+S weights) at baseline (WT n = 8, R213G n = 6) after 35 days of HPX (WT n = 7, R213G n = 8). (**D**) Representative lung α-sma immunostaining (brown signal) with counterstain by hematoxylin (blue) after 35 days of HPX. Bar = 50 microns. Arrows

indicate muscularized small vessels identified by positive α-sma immunostaining. (**E**) Quantitation of muscularized small vessels (< 50 microns) in a 10× field at baseline (WT n = 5, R213G n = 6) and after 35 days of HPX (WT n = 4, R213G n = 5). (**F**) Collagen visualized by TPE-SHG in representative unstained tissue sections. Collagen (red signal), tissue autofluorescence (green signal). (**G**) Quantification of collagen standardized for vessel size (n= 6 for all groups). Data are shown as mean ± S.E. * $P < 0.01$ for WT compared to R213G samples under identical conditions. # $P < 0.01$ for NX compared to HPX.

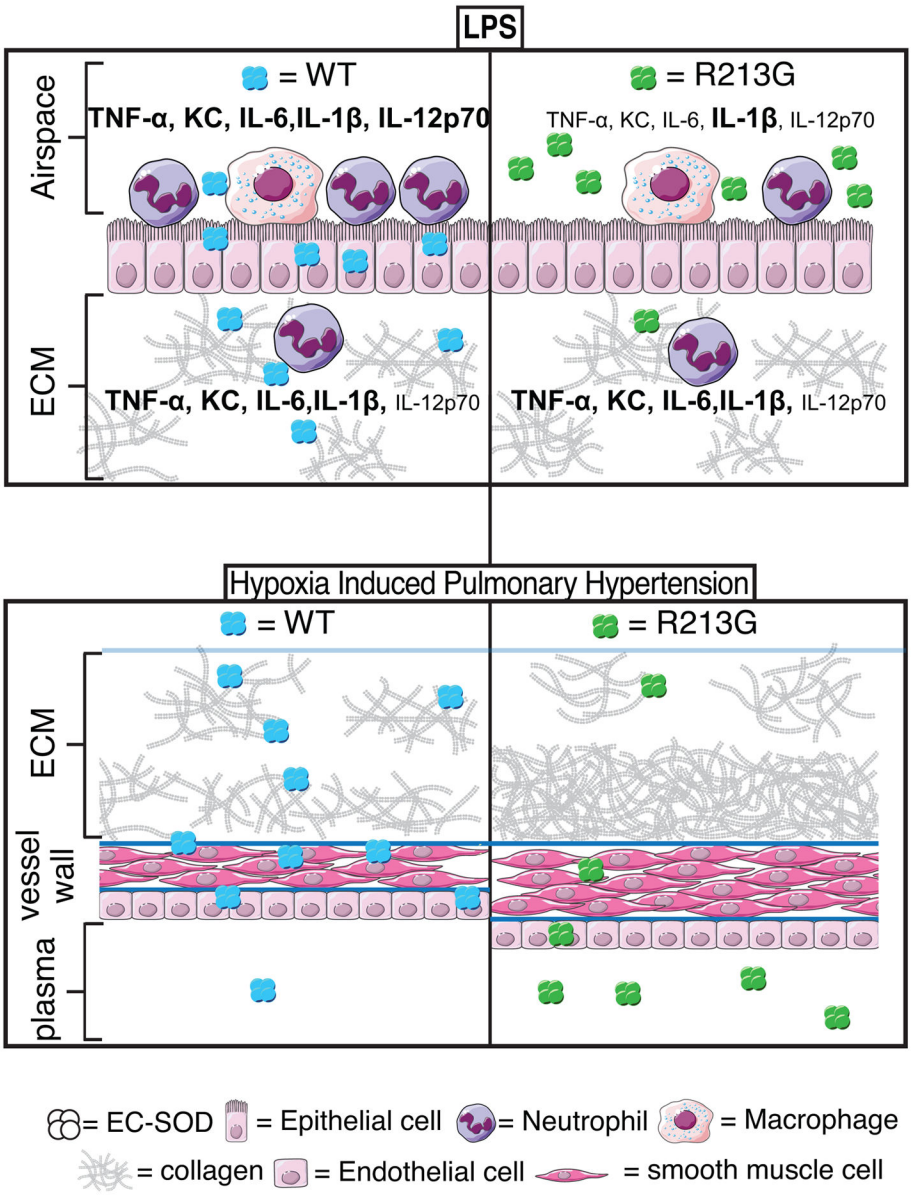

Figure 4.

Schematic demonstrating the change in distribution of EC-SOD associated with the R213 SNP. The consequence of the change in distribution is a reduction in susceptibility to inflammation from lipopolysaccharide (LPS) and increased susceptibility to vascular disease (hypoxic pulmonary hypertension and remodeling).